Magn Reson Med Sci 2018; 17; 168–173
doi:10.2463/mrms.mp.2017-0047
Published Online: August 16, 2017

MAJOR PAPER

Histological Grading of Hepatocellular Carcinomas with Intravoxel Incoherent Motion Diffusion-weighted Imaging: Inconsistent Results Depending on the Fitting Method

Shintaro Ichikawa[1], Utaroh Motosugi[1*], Diego Hernando[2], Hiroyuki Morisaka[3], Nobuyuki Enomoto[4], Masanori Matsuda[5], and Hiroshi Onishi[1]

Purpose: To compare the abilities of three intravoxel incoherent motion (IVIM) imaging approximation methods to discriminate the histological grade of hepatocellular carcinomas (HCCs).

Methods: Fifty-eight patients (60 HCCs) underwent IVIM imaging with 11 *b*-values (0–1000 s/mm^2). Slow (*D*) and fast diffusion coefficients (D^*) and the perfusion fraction (*f*) were calculated for the HCCs using the mean signal intensities in regions of interest drawn by two radiologists. Three approximation methods were used. First, all three parameters were obtained simultaneously using non-linear fitting (method A). Second, *D* was obtained using linear fitting (*b* = 500 and 1000), followed by non-linear fitting for D^* and *f* (method B). Third, *D* was obtained by linear fitting, *f* was obtained using the regression line intersection and signals at *b* = 0, and non-linear fitting was used for D^* (method C). A receiver operating characteristic analysis was performed to reveal the abilities of these methods to distinguish poorly-differentiated from well-to-moderately-differentiated HCCs. Inter-reader agreements were assessed using intraclass correlation coefficients (ICCs).

Results: The measurements of *D*, D^*, and *f* in methods B and C (Az-value, 0.658–0.881) had better discrimination abilities than did those in method A (Az-value, 0.527–0.607). The ICCs of *D* and *f* were good to excellent (0.639–0.835) with all methods. The ICCs of D^* were moderate with methods B (0.580) and C (0.463) and good with method A (0.705).

Conclusion: The IVIM parameters may vary depending on the fitting methods, and therefore, further technical refinement may be needed.

Keywords: *hepatocellular carcinoma, histological grade, intravoxel incoherent motion, magnetic resonance imaging*

Introduction

The histological grade of a hepatocellular carcinoma (HCC) is one of the most predictive factors of recurrence and survival after surgery in patients with HCCs.[1,2] High-grade HCCs are associated with a lower survival rate compared to low-to-moderate-grade HCCs.[3] In general, hepatologists do not perform biopsy for HCCs before treatment, particularly if an imaging-based diagnosis has been made, in order to avoid spreading the tumor cells throughout the peritoneal cavity. Therefore, imaging-based predictions of the histological grade would be useful for establishing the proper management strategy for HCCs.

Several researchers have attempted to evaluate the histological grade of HCCs with MRI, for instance by using the signal intensity on T_2-weighted images,[4] enhancement patterns on gadoxetic acid-enhanced MR images,[5,6] or the apparent diffusion coefficient (ADC) value measured using diffusion-weighted images (DWI).[7,8] It should be noted that the ADC value is typically reduced in malignant lesions, especially in high-grade malignancies such as poorly differentiated HCCs. However, microcirculation or perfusion-related diffusion in the tumor, as well as true molecular diffusion, can affect the signal changes in DWI and decrease the ADC value. If both perfusion-related diffusion and true molecular (proton) diffusion decrease the ADC value of malignant lesions, then it

[1]Department of Radiology, University of Yamanashi, 1110 Shimokato, Chuo-shi, Yamanashi 409-3898, Japan
[2]Department of Radiology, University of Wisconsin, Madison, WI, USA
[3]Department of Diagnostic Radiology, Saitama Medical University International Medical Center, Saitama, Japan
[4]First Department of Internal Medicine, University of Yamanashi, Yamanashi, Japan
[5]First Department of Surgery, University of Yamanashi, Yamanashi, Japan
*Corresponding author, Phone: +81-55-273-1111, Fax: +81-55-273-6744, E-mail: umotosugi@nifty.com

This paper was presented at European Society of Gastrointestinal and Abdominal Radiology (ESGAR) 2016 annual meeting in June 2016.

Received: April 5, 2017 | Accepted: July 5, 2017

is essential to determine which of these two factors more strongly affects the ADC value and which is the most relevant for distinguishing the histological grade of HCCs.

Intravoxel incoherent motion (IVIM) imaging is a technique used to estimate the diffusion that is associated with tissue perfusion and is based on diffusion parameters that are calculated using multi-b-value DWI. The IVIM model using bi-exponential fitting was first described by Le Bihan et al. in 1986.[9] Recent advances in MRI have facilitated the application of IVIM imaging in the separate estimation of tissue perfusion-related diffusion and the diffusion of protons in abdominal organs. In addition, several studies have demonstrated the utility of IVIM imaging for distinguishing between malignant and benign focal liver lesions[10,11] and for determining the histological grade of HCCs.[12]

Although the basic concept of IVIM imaging is simple, there are still some inconsistencies in the fitting methods. Indeed, the calculated results can vary depending on the fitting methods used to estimate the bi-exponential curve of IVIM.[10,13,14] Currently, little is known about the effects that different approximation methods would have on the diagnostic ability and/or reproducibility of IVIM imaging for liver lesions.[15,16] Hence, the purpose of this study was to compare the repeatability and discrimination abilities of three different approximation methods that were applied to IVIM images in order to distinguish the histological grade of HCCs.

Materials and Methods

Patients

This retrospective study was performed in accordance with the principles outlined in the Declaration of Helsinki, and was approved by the relevant institutional review board, which waived the requirement for informed patient consent owing to the retrospective nature of the study. Between May 2012 and November 2014, 1928 consecutive patients underwent abdominal MRI with IVIM for liver investigations. This data were matched with information from a pathological database in order to find patients with chronic liver disease who had surgically confirmed HCCs that were >15 mm in diameter. Although 61 patients were identified, three patients were excluded because a measurable IVIM images were not available owing to motion artifacts. Finally, we included 60 nodules (mean diameter: 39 mm, range: 16–238 mm) in 58 patients (42 men, 16 women; age range: 46 to 88 years, mean age: 70.0 ± 10.2 years) in the study (Fig. 1). There were no patients who had previous treatment for the nodules. The histological grades of the HCCs were retrieved from the official report by one of the two pathologists at our institution (17 and 20 years of experience, respectively) both of whom were blinded to the IVIM results. The final histological differentiation of the HCCs were well differentiated (n = 17), moderately differentiated (n = 30), or poorly differentiated (n = 13). The etiologies of chronic liver disease were hepatitis C (n = 28), hepatitis B (n = 12), alcoholic steatohepatitis (n = 7), nonalcoholic steatohepatitis (n = 3), schistosomiasis (n = 3), and uncertain liver disease with an elevated liver enzyme level (n = 5).

IVIM imaging

Magnetic resonance imaging was performed using a superconducting magnet operating at 3 Tesla (Discovery 750; GE Medical Systems, Waukesha, WI) with a 32-channel phased-array coil. IVIM images were acquired in the transverse plane by respiratory triggered fat-saturated spin echo-echo planar imaging. The MR parameters were as follows: TR/TE, 3000–4000/54 ms; flip angle, 90º; matrix, 128 × 128; FOV, 40 × 40 cm; section thickness/intersection gap, 7/3 mm; number of slices, 16 slices for each b-value; parallel imaging factor, 2; number of excitations, 3; and acquisition time, 120–180 s. Motion-proving gradient pulses were concurrently applied in three directions (x, y, and z). The following 11 b-values were used: 0, 10, 20, 30, 40, 50, 80, 100, 200, 500, and 1000 s/mm^2.[17] Three diffusivity values were set as follows: the slow diffusion coefficient, which is non-perfusion related but indicates the molecular diffusion-related diffusivity (true diffusion coefficient [D]; $\times 10^{-3}$ mm^2/s) and true molecular diffusion; the fast diffusion coefficient, which is related to perfusion in micro-vessels (diffusion coefficient for perfusion [D^*]; $\times 10^{-3}$

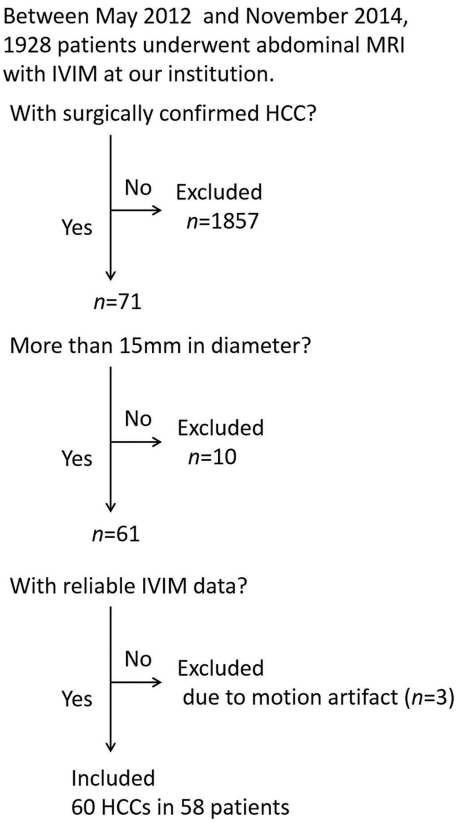

Fig. 1 Inclusion criteria applied prior to the enrollment of study participants. IVIM, intravoxel incoherent motion; HCC, hepatocellular carcinoma.

mm^2/s); and the perfusion-related diffusion fraction (perfusion fraction [*f*]; %), which represents the fractional volume occupied in the voxel by flowing spins.

To obtain these values, two radiologists (S.I. and H.M.), each with 9 years of experience in abdominal radiology, who were blinded to the histopathological data manually placed ROIs on the entire lesion using a workstation (SYNAPSE VINCENT, FUJIFILM Medical, Tokyo, Japan). In the case of larger lesions showing solid components with inhomogeneous signal intensity, ROIs were positioned by avoiding areas of necrosis and hemorrhage by reference to T_2-weighted images. First, the ROIs were placed on the ADC map (Fig. 2), and then the ROIs were automatically copied to images of each b-value to retrieve the signal intensity decay of the lesion. The following three approximation methods were used for estimating D, D^*, and f based on the signal intensity of each b-value. In method A, we obtained all three parameters (D, D^*, and f) simultaneously using non-linear fitting; in method B, we obtained D first using images with b = 500 and 1000 s/mm^2 by linear fitting, followed by non-linear fitting for D^* and f; and in method C, we obtained D as described in method B, and then obtained f using the intersection of the regression line and signals of b = 0 s/mm^2 and non-linear fitting for D^* only. Calculations of these approximations were performed using Matlab (The MathWorks, Inc., Natick, MA, USA).

Statistical analysis

A receiver operating characteristic analysis was performed to discriminate poorly differentiated from well-to-moderately differentiated HCCs. Inter-reader agreement was assessed using the intraclass correlation coefficient (ICC). An ICC value (r) > 0.8 was considered excellent agreement, $0.6 < r \leq 0.8$ was deemed good, $0.4 < r \leq 0.6$ was moderate, $0.2 < r \leq 0.4$ was fair, and ≤ 0.2 was considered poor agreement. We analyzed all statistics using the IBM SPSS software (Ver. 22.0; IBM Corp., Armonk, NY, USA). The statistical significance level was set at $P < 0.05$.

Results

The three diffusivity values calculated by each method and reader are summarized in Table 1. No significant differences were identified between well-to-moderately differentiated and poorly differentiated HCCs for any of the three diffusivity values calculated by method A (P = 0.2399–0.9072). The D and D^* values calculated by methods B and C for poorly differentiated HCCs were significantly lower than were those for well-to-moderately differentiated HCCs ($P \leq$ 0.0001–0.0366). In contrast, the f values calculated by methods B and C for poorly differentiated HCCs were significantly higher than were those for well-to-moderately differentiated HCCs (P = 0.0016–0.0279), except for the results of reader 2 when using method B (P = 0.0834). Methods B and C (Az value, 0.701–0.881) had better HCC grade discrimination abilities compared to method A (Az value, 0.527–0.607) for all three diffusivity values (Table 2).

The inter-reader ICC values of D and f were good to excellent (r = 0.639–0.835) with all methods. The ICC values of D^* were moderate with methods B (r = 0.580) and C (r = 0.463) and good with method A (r = 0.705) (Table 3).

Discussion

In this study, all IVIM parameters (D, D^*, and f) were significantly different between well-to-moderately differentiated and poorly differentiated HCCs when estimation methods B and C were used, but not when method A was used. In other words, different methods led to different results even though the same data were used.

In a previous study that focused on differentiating the HCC grade using IVIM imaging, the D values were lower in high-grade HCCs than they were in low-grade HCCs.[12] In our study, the D and D^* values were lower in poorly differentiated HCCs than they were in well-to-moderately differentiated HCCs. Moreover, the receiver operating characteristic analysis showed that the Az values of D were higher

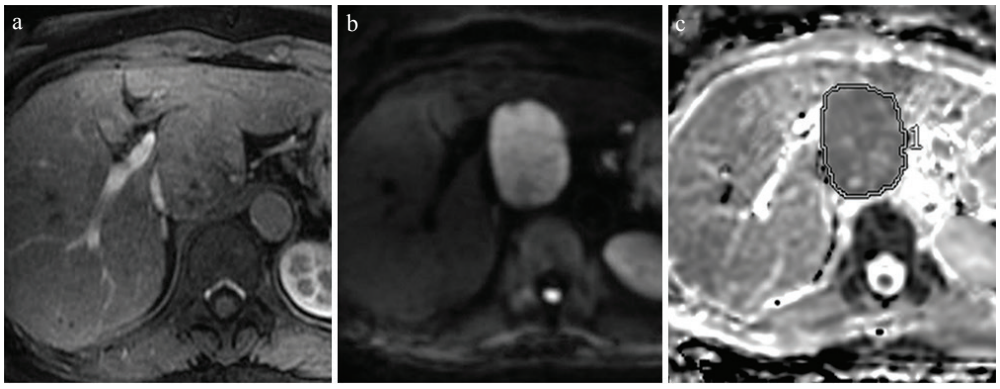

Fig. 2 Rules for ROI placement, as demonstrated on representative images from a 69-year-old woman with hepatitis B. (**a**) Hepatic arterial-phase images show a slightly enhanced tumor at the caudate lobe. (**b**) This nodule shows high intensity on a diffusion-weighted image (b = 1000 s/mm). (**c**) We manually placed ROIs on the entire lesion on apparent diffusion coefficient (ADC) maps using SYNAPSE VINCENT software (FUJIFILM Medical, Tokyo, Japan).

Table 1. The three diffusivity values calculated by each method and reader

	Well-to-moderately differentiated HCC	Poorly differentiated HCC	*P* value
Method A, reader 1			
D (×10^{-3} mm^2/s)	1.05 (1.03, 0.72–1.97)	1.00 (0.95, 0.81–1.37)	0.3649
D* (×10^{-3} mm^2/s)	551.0 (62.5, 5.0–3553.4)	303.1 (46.4, 5.0–3410.3)	0.3990
f (%)	12.7 (11.5, 0–31.1)	12.8 (11.3, 5.9–22.1)	0.6864
reader 2			
D (×10^{-3} mm^2/s)	1.04 (1.04, 0.58–1.97)	0.97 (0.92, 0.76–1.34)	0.2399
D* (×10^{-3} mm^2/s)	538.6 (44.6, 5.0–4181.4)	325.0 (47.2, 5.3–3522.7)	0.7672
f (%)	12.8 (13.2, 0–32.3)	12.9 (12.5, 5.0–24.7)	0.9072
Method B, reader 1			
D (×10^{-3} mm^2/s)	0.95 (0.96, 0.70–1.28)	0.72 (0.71, 0.55–0.97)	<0.0001†
D* (×10^{-3} mm^2/s)	228.5 (30.7, 5.0–3904.2)	19.0 (15.7, 5.0–77.9)	0.0211†
f (%)	16.5 (15.8, 0–53.8)	23.6 (23.4, 8.9–50.2)	0.0232†
reader 2			
D (×10^{-3} mm^2/s)	0.95 (0.97, 0.65–1.34)	0.75 (0.76, 0.54–0.97)	0.0005†
D* (×10^{-3} mm^2/s)	323.2 (31.4, 5.0–2642.7)	22.6 (13.9, 5.1–78.5)	0.0366†
f (%)	15.7 (15.9, 0–53.3)	21.7 (18.7, 8.2–50.7)	0.0834
Method C, reader 1			
D (×10^{-3} mm^2/s)	0.95 (0.96, 0.70–1.28)	0.72 (0.71, 0.55–0.97)	<0.0001†
D* (×10^{-3} mm^2/s)	204.6 (15.8, 0–2214.1)	7.88 (6.47, 5.0–12.3)	0.0004†
f (%)	18.3 (17.9, 0–55.7)	29.2 (31.6, 9.7–54.3)	0.0016††
reader 2			
D (×10^{-3} mm^2/s)	0.95 (0.97, 0.65–1.34)	0.75 (0.76, 0.54–0.97)	0.0005†
D* (×10^{-3} mm^2/s)	155.1 (14.1, 0–2292.9)	8.71 (7.96, 5.0–14.6)	0.0192†
f (%)	17.8 (16.7, 0–55.7)	25.9 (24.6, 11.5–54.5)	0.0279††

Statistical analyses were performed using the Wilcoxon test. Data are presented as the mean (median, range). HCC, hepatocellular carcinoma; *D*, true diffusion coefficient; *D**, diffusion coefficient for perfusion; *f*, perfusion fraction. †, The *D* and *D** values of poorly differentiated HCCs were lower than were those of well-to-moderately differentiated HCCs ($P < 0.05$); ††, The *f* value of poorly differentiated HCCs was higher than was that of well-to-moderately differentiated HCCs ($P < 0.05$).

Table 2. The Az values for the HCC grade discrimination ability (well-to-moderately differentiated vs. poorly differentiated)

	D (×10^{-3} mm^2/s)	*D** (×10^{-3} mm^2/s)	*f* (%)
Method A			
reader 1	0.583 (0.398–0.747)	0.577 (0.406–0.731)	0.534 (0.364–0.701)
reader 2	0.607 (0.432–0.759)	0.527 (0.361–0.688)	0.489 (0.312–0.669)
Method B			
reader 1	0.881 (0.738–0.951)	0.710 (0.548–0.832)	0.707 (0.523–0.842)
reader 2	0.819 (0.667–0.911)	0.691 (0.526–0.818)	0.658 (0.470–0.807)
Method C			
reader 1	0.881 (0.738–0.951)	0.825 (0.696–0.907)	0.787 (0.599–0.902)
reader 2	0.819 (0.667–0.911)	0.714 (0.575–0.821)	0.701 (0.536–0.826)

Data are presented with the 95% confidence interval in parentheses. HCC, hepatocellular carcinoma; *D*, true diffusion coefficient; *D**, diffusion coefficient for perfusion; *f*, perfusion fraction.

Table 3. Inter-reader intraclass correlation coefficients (ICC)

	D ($\times 10^{-3}$ mm^2/s)	D^* ($\times 10^{-3}$ mm^2/s)	f (%)
Method A	0.818 (0.712–0.887)	0.705 (0.551–0.813)	0.639 (0.461–0.767)
Method B	0.785 (0.664–0.866)	0.580 (0.384–0.726)	0.801 (0.687–0.876)
Method C	0.785 (0.664–0.866)	0.463 (0.239–0.641)	0.835 (0.738–0.898)

Data are presented with the 95% confidence interval in parentheses. D, true diffusion coefficient; D^*, diffusion coefficient for perfusion; f, perfusion fraction.

than were those of D^* for distinguishing poorly differentiated HCCs from well-to-moderately differentiated HCCs. This result suggests that the D value is a more reliable parameter than is the D^* value in terms of tumor grade determination, which is consistent with the findings of the abovementioned study.[12] Therefore, restricted molecular diffusion is probably a stronger indicator of poorly differentiated HCCs than is perfusion. This may at least be attributable to the fact that the vascularity is the highest for moderately differentiated HCC, whereas those for well and poorly differentiated HCC are relatively low, on the other hand, the cellular density or ADC values has been known to gradually increase from well differentiated to poorly differentiated HCC.

Interestingly, these results were only observed in methods B and C. Despite the increasing use of IVIM imaging in research and clinics, no consensus exists regarding the optimal estimation approach for the IVIM model.[18,19] Since the inter-reader ICC for the D value obtained using method A (0.818) was as high as the values obtained using methods B and C (0.785 and 0.785, respectively), the worse discrimination ability of method A was probably related to acquisition variability. As method A estimated three unknowns at once using non-linear fitting, the solution may be unstable. On the other hand, methods B and C commonly used linear fitting for the D value, thus the fitting would be robust even though some errors might have occurred during image acquisition.

Similar to the findings of a previous study,[16] our study also showed that the inter-reader reproducibility of D was better than that of f and D^*. The poor reproducibility of D^* may be related to unstable signal acquisition or fitting uncertainty, as demonstrated in recent studies.[19,20]

Our study was mainly limited by its retrospective design and the small sample size. A prospective study with a larger cohort would be necessary to confirm the usefulness of the IVIM parameters for distinguishing poorly differentiated HCCs from other HCC grades and to establish the advantages of estimation methods that utilize linear fitting. Instability of D^* is also limitation. Unfortunately, no rigid solution has been proposed for addressing the instability of D^* measurements in the IVIM model, thus additional studies are needed.

Conclusion

The IVIM parameters may vary depending on the fitting methods, further technical refinement may be needed.

Acknowledgment

We thank Tetsuya Wakayama from GE Healthcare for the technical support.

Conflicts of Interest

The authors declare that they have no conflict of interest.

References

1. Jonas S, Bechstein WO, Steinmüller T, et al. Vascular invasion and histopathologic grading determine outcome after liver transplantation for hepatocellular carcinoma in cirrhosis. Hepatology 2001; 33:1080–1086.
2. Zhou L, Rui JA, Wang SB, et al. Factors predictive for long-term survival of male patients with hepatocellular carcinoma after curative resection. J Surg Oncol 2007; 95:298–303.
3. Zhou L, Rui JA, Ye DX, Wang SB, Chen SG, Qu Q. Edmondson-Steiner grading increases the predictive efficiency of TNM staging for long-term survival of patients with hepatocellular carcinoma after curative resection. World J Surg 2008; 32:1748–1756.
4. Iwasa Y, Kitazume Y, Tateishi U, et al. Hepatocellular carcinoma histological grade prediction: A quantitative comparison of diffusion-weighted, T2-weighted, and hepatobiliary-phase magnetic resonance imaging. J Comput Assist Tomogr 2016; 40:463–470.
5. Choi JY, Kim MJ, Park YN, et al. Gadoxetate disodium-enhanced hepatobiliary phase MRI of hepatocellular carcinoma: correlation with histological characteristics. AJR Am J Roentgenol 2011; 197:399–405.
6. Schelhorn J, Best J, Dechêne A, et al. Evaluation of combined Gd-EOB-DTPA and gadobutrol magnetic resonance imaging for the prediction of hepatocellular carcinoma grading. Acta Radiol 2016; 57:932–938.
7. Chen J, Wu M, Liu R, Li S, Gao R, Song B. Preoperative evaluation of the histological grade of hepatocellular carcinoma with diffusion-weighted imaging: a meta-analysis. PLoS ONE 2015; 10:e0117661.
8. Guo W, Zhao S, Yang Y, Shao G. Histological grade of hepatocellular carcinoma predicted by quantitative diffusion-weighted imaging. Int J Clin Exp Med 2015; 8:4164–4169.
9. Le Bihan D, Breton E, Lallemand D, Grenier P, Cabanis E, Laval-Jeantet M. MR imaging of intravoxel incoherent motions: application to diffusion and perfusion in neurologic disorders. Radiology 1986; 161:401–407.

10. Ichikawa S, Motosugi U, Ichikawa T, Sano K, Morisaka H, Araki T. Intravoxel incoherent motion imaging of focal hepatic lesions. J Magn Reson Imaging 2013; 37:1371–1376.
11. Yoon JH, Lee JM, Yu MH, Kiefer B, Han JK, Choi BI. Evaluation of hepatic focal lesions using diffusion-weighted MR imaging: comparison of apparent diffusion coefficient and intravoxel incoherent motion-derived parameters. J Magn Reson Imaging 2014; 39:276–285.
12. Woo S, Lee JM, Yoon JH, Joo I, Han JK, Choi BI. Intravoxel incoherent motion diffusion-weighted MR imaging of hepatocellular carcinoma: correlation with enhancement degree and histologic grade. Radiology 2014; 270:758–767.
13. Pasquinelli F, Belli G, Mazzoni LN, Grazioli L, Colagrande S. Magnetic resonance diffusion-weighted imaging: quantitative evaluation of age-related changes in healthy liver parenchyma. Magn Reson Imaging 2011; 29:805–812.
14. Neil JJ, Bretthorst GL. On the use of Bayesian probability theory for analysis of exponential decay data: an example taken from intravoxel incoherent motion experiments. Magn Reson Med 1993; 29:642–647.
15. Andreou A, Koh DM, Collins DJ, et al. Measurement reproducibility of perfusion fraction and pseudodiffusion coefficient derived by intravoxel incoherent motion diffusion-weighted MR imaging in normal liver and metastases. Eur Radiol 2013; 23:428–434.
16. Kakite S, Dyvorne H, Besa C, et al. Hepatocellular carcinoma: short-term reproducibility of apparent diffusion coefficient and intravoxel incoherent motion parameters at 3.0T. J Magn Reson Imaging 2015; 41:149–156.
17. Lemke A, Stieltjes B, Schad LR, Laun FB. Toward an optimal distribution of b values for intravoxel incoherent motion imaging. Magn Reson Imaging 2011; 29:766–776.
18. Merisaari H, Movahedi P, Perez IM, et al. Fitting methods for intravoxel incoherent motion imaging of prostate cancer on region of interest level: repeatability and gleason score prediction. Magn Reson Med 2017; 77:1249–1264.
19. Cho GY, Moy L, Zhang JL, et al. Comparison of fitting methods and b-value sampling strategies for intravoxel incoherent motion in breast cancer. Magn Reson Med 2015; 74:1077–1085.
20. Dyvorne HA, Galea N, Nevers T, et al. Diffusion-weighted imaging of the liver with multiple b values: effect of diffusion gradient polarity and breathing acquisition on image quality and intravoxel incoherent motion parameters—a pilot study. Radiology 2013; 266:920–929.